Diffusion and phase diagram of an electron-hole bilayer: A molecular dynamics study

S. Ranganathan
Department of Physics, Royal Military College of Canada, Kingston, Ontario, Canada K7K 7B4

R. E. Johnson
Department of Mathematics and Computer Science, Royal Military College of Canada, Kingston, Ontario, Canada K7K 7B4

(Received 12 January 2007; revised manuscript received 19 February 2007; published 11 April 2007)

Molecular dynamics simulations of a classical, symmetric electron-hole bilayer for various values of the coupling strength Γ and interlayer separation distance d have been performed. We have analyzed the pair correlation functions, the static structure factor, and the diffusion coefficient in this study. As d is decreased, diffusion goes through a minimum and then increases very rapidly; its behavior at small d can be attributed to the formation of stable, weakly interacting electron-hole dipoles. We have constructed the phase diagram in the Γ-d plane based on the amplitude of the main peak of the intralayer static structure factor and the diffusion coefficient. It is found that a solid phase is not possible for d less than about 0.5 for any Γ, nor for Γ less than about 100 for any d. Our phase diagram, obtained using a different methodology, is in good agreement with the one in the literature.

DOI: 10.1103/PhysRevB.75.155314 PACS number(s): 71.10.Hf, 68.65.Ac, 52.65.Yy

I. INTRODUCTION

Layered structures in which each layer is made up of identical charged particles and immersed in a uniform neutralizing background of the opposite charge have been a subject of considerable research interest over the past decade. This neutral system is referred to as one-component plasma (OCP). Classical bilayer systems made up of charges of the same sign, which we will refer to as an electron-electron (e-e) bilayer, have been investigated through molecular dynamics (MD)[1–5] and theoretical models.[6–8] Properties of such systems depend only on two parameters: the interlayer separation d and the classical plasma coupling parameter $\Gamma = \frac{e^2}{ak_BT}$, the ratio of the average potential energy to the average kinetic energy per particle; $a=(n\pi)^{-1/2}$ is the Wigner-Seitz (WS) radius, with n being the areal density, k_B the Boltzmann constant, e the electronic charge, and T the temperature. Such systems have been shown to exhibit a rich variety of interesting features as a function of d: MD studies have shown, for example, that the system exhibits a series of abrupt structural changes, the diffusion coefficient goes through a minimum,[2] and the phase changes from a liquid to a solid and back to a liquid.[5,9] On the other hand, the electron-hole (e-h) system in which the two layers are made up of charged particles of opposite charges behaves somewhat differently because of the Coulomb attraction between the electrons and the holes which naturally binds them to form dipoles especially at small interlayer separations. This phenomenon would contribute significantly to the structural and dynamical properties of such a system. Previous computer simulation studies of the e-h system have examined the pair distribution function[10] and thereby produced a phase diagram.[11] In this study, we analyze the static structure factor and the diffusion coefficient to arrive at a phase diagram. The criterion for freezing based on the peak value of the static structure factor has been applied to other systems in two-dimensions[12,13] and to an e-e bilayer,[5] and seems to be universally valid.

II. SIMULATION DETAILS

The system to be simulated is a bilayer consisting of electrons in one layer and holes (positrons) in the other, interacting through a $1/r$ Coulomb potential. The particles are distributed in two parallel planes separated by a distance d; each particle is constrained to move only in the plane of its original distribution. Charge neutrality in each plane is guaranteed by embedding the particles in a uniform background of opposite charge. The thermodynamic state of the system is entirely specified by Γ and d. Only symmetric bilayers, in which the density of the particles is the same in both layers, are considered in this study.

The details of the simulation and the extended Ewald sum technique have been described in our earlier paper.[14] For the sake of completeness, we include some of the essential features of our simulation here. The dynamics in our MD simulation needs the force, and as an example, the force on any one particle due to all particles in the same plane and the other plane is given by

$$\begin{aligned}\vec{F}(\vec{r}_1) = \frac{2\pi}{L^2}\sum_{\vec{g}\neq\vec{0}}\vec{g}\Bigg\{&\frac{1}{g}\,\mathrm{erfc}\left(\frac{g}{2\alpha}\right)\sum_{j=2}^{N}\sin[\vec{g}\circ(\vec{r}_1-\vec{r}_j)]\\&-\psi(g;\kappa,d)\sum_{j=1}^{N}\sin[\vec{g}\circ(\vec{r}_1-\vec{\rho}_j)]\Bigg\}\\&+\sum_{\vec{p}}\sum_{j=1}^{N}{}'\frac{\vec{s}_{1j}}{|\vec{s}_{1j}|^3}\Bigg\{\mathrm{erfc}(\alpha|\vec{s}_{1j}|)+\alpha|\vec{s}_{1j}|\frac{2}{\sqrt{\pi}}\\&\times\exp(-\alpha^2|\vec{s}_{1j}|^2)\Bigg\}-\sum_{\vec{p}}\sum_{j=1}^{N}\frac{\vec{d}_{1j}}{|\vec{d}_{1j}|^3}\Bigg\{\mathrm{erfc}(\kappa|\vec{d}_{1j}|)\\&+\kappa|\vec{d}_{1j}|\frac{2}{\sqrt{\pi}}\exp(-\kappa^2|\vec{d}_{1j}|^2)\Bigg\}\end{aligned}\tag{1}$$

with

$$\psi(g;\kappa,d) = \int_0^\infty dr \frac{r}{\sqrt{r^2+d^2}} \operatorname{erf}(\kappa\sqrt{r^2+d^2}) J_0(gr)$$
$$= \frac{1}{2g}\left[e^{gd} \operatorname{erfc}\left(\frac{g}{2\kappa} + \kappa d\right) + e^{-gd} \operatorname{erfc}\left(\frac{g}{2\kappa} - \kappa d\right)\right], \quad (2)$$

$\vec{s}_{1j}=\vec{r}_1-\vec{r}_j+\vec{p}$ and $\vec{d}_{1j}=\vec{r}_1-\vec{\rho}_j+\vec{d}+\vec{p}$; $\vec{r}_i$ denotes the position of the ith particle in the same (x,y) plane and $\vec{\rho}_j$ denotes the position of the jth particle in the other (x,y) plane, and the planes are separated by a distance d along the z axis; L is the length of the square simulation cell and N is the number of particles in each cell. Each sum over $\vec{p}$ is a sum over integers k_1 and k_2 with $\vec{p}=L(k_1,k_2)$; the prime in the second term implies that if $\vec{p}=\vec{0}$, the $j=1$ term is to be omitted. The sum over $\vec{g}$ is a sum over integers λ_1,λ_2 with $\vec{g}=\frac{2\pi}{L}(\lambda_1,\lambda_2)$. The parameters α and κ are to be so chosen that both series in (1) converge rapidly; our analysis indicates that an optimum choice for both of these parameters is $8/L$. Acceptable accuracy for the sum in the first term of (1) can be obtained using $|\vec{\lambda}|$ as small as 5; however we used $|\vec{\lambda}|<10$ in the calculations presented here. This is sufficiently large that only the $\vec{p}=\vec{0}$ terms in the p-summation in (1) need to be retained, implying that the real-space terms vanish at a distance corresponding to half-the-box length. All quantities involved are in dimensionless units: distance in units of WS radius a, time in units of $\tau=\sqrt{\frac{ma^3}{e^2}}$ and energies in units of e^2/a. The two layers have the same surface density and the basic cell is a square with side length $L=\left(\frac{N}{na^2}\right)^{1/2}$, containing $N=512$ electrons in one layer and the same number of positrons in the other layer. Since a is the unit of length, the density in each layer takes the value $1/\pi$. Our MD simulation provides the position vector $\vec{r}_k(t)=[x_k(t),y_k(t)]$ and the velocity vector $\vec{v}_k(t)=[v_{kx}(t),v_{ky}(t)]$ for $k=1$ to 512 particles in each of the two layers and for 10 000 times separated by a time step of 0.06. This data is then used to obtain the various correlation functions. Simulations were performed for selected values of Γ from 50 to 170 and d from 0.1 to 3.0.

III. RESULTS

The MD data for the position vector and the velocity vector for any specific value of Γ and d can then be used to obtain the corresponding static or dynamic correlation functions. The quantities of interest in this study are the intralayer and interlayer pair correlation functions $g_{11}(r)$ and $g_{12}(r)$, respectively, the Fourier transform $S_{11}(q)$ of $g_{11}(r)$, and the mean-square displacement $\langle\Delta r^2(t)\rangle$ from which the diffusion coefficient D was obtained. All of these quantities can be obtained from the position vector data set alone. The relevant formulas are

$$g(r) = \frac{\langle n(r)\rangle}{2\pi r \Delta r n}, \quad (3)$$

$$S_{11}(q) = 1 + 2\pi n \int_0^\infty [g_{11}(r)-1] r J_0(qr) dr, \quad (4)$$

$$\langle\Delta r^2(t)\rangle = \frac{1}{N}\left\langle \sum_{j=1}^{N} |\vec{r}_j(t)-\vec{r}_j(0)|^2 \right\rangle, \quad (5)$$

$$D = \lim_{t\to\infty} \frac{\langle\Delta r^2(t)\rangle}{4t} = \lim_{t\to\infty} \frac{1}{4}\frac{d}{dt}\langle\Delta r^2(t)\rangle, \quad (6)$$

where $\langle n(r)\rangle$ is the average number of particles in one of the layers in an annulus of radius r and thickness Δr, centered at a given particle and J_0 is the Bessel function of order zero.

A. Pair correlation functions

We have calculated the pair distribution functions (pdf) $g_{11}(r)$ and $g_{12}(r)$ for a number of values of Γ and d. It is only to be expected that because of the Coulomb attraction, the pdf will be quite different from that of an e-e bilayer. Figure 1 shows the graphs for $\Gamma=150$ and some selected values of d. These are in agreement with those of Hartmann *et al.*[11] whose results are based on Monte Carlo (MC) simulations. Some of the salient features: (a) $g_{11}(r)$ and $g_{12}(r)$ graphs are almost identical for a range of d from very small to about 1.5, except for the very sharp peak near $r=0$ for $g_{12}(r)$ and small differences in the height of the first peak. The former is due to the very strong electron-hole attraction leading to the formation of dipoles. (b) At d less than 0.3, both pdf show a slightly enhanced first peak with no long range order, implying that the system behaves much like a dilute gas, even though the coupling parameter Γ is at a very high value of 150. (c) At $d=0.8$, both pdf exhibit a sharp first peak and a long range order indicative of a liquidlike structure. (d) At $d=1.2$, one sees the initial signs of the formation of a shoulder in both pdf, which becomes very evident at $d=1.5$. It has been suggested that the first indication of a shoulder in $g_{11}(r)$ is indicative of the onset of freezing.[12] (e) For d greater than 2, $g_{12}(r)$ loses its long range character and the interlayer correlation is no longer appreciable and around $d=2.5$, the two layers behave independently. Since Γ is 150, $g_{11}(r)$ reveals a strong first peak and very long oscillations, indicative of an almost solid-like structure.

The height of the peak of $g_{12}(r\sim 0)$ increases dramatically, by orders of magnitude, as d decreases; typically it goes from around 1 for $d=2$ to 10^5 or higher for $d=0.2$. This behavior can be attributed to the increased Coulomb attraction between the electron and the hole as the dipolelike structure sets in. Hartmann *et al.*[11] have analyzed their data on the height $g_{12}(r=0)$ as a function of d, and it shows a d^{-3} dependence for $0.1<d<1$. Our results agree with their data, but only for $d>0.4$; for smaller d, our results seem to indicate a much faster rate of increase. A detailed and careful analysis is required to resolve the d dependence. The problem is complicated since the electron and hole positions practically coincide for small d; hence an acceptable value of Δr (which must be quite small) and the convergence of the $g_{12}(r=0)$ values become somewhat difficult to attain. We intend to study the dependence of the peak height on not only d but also Γ in a future paper.

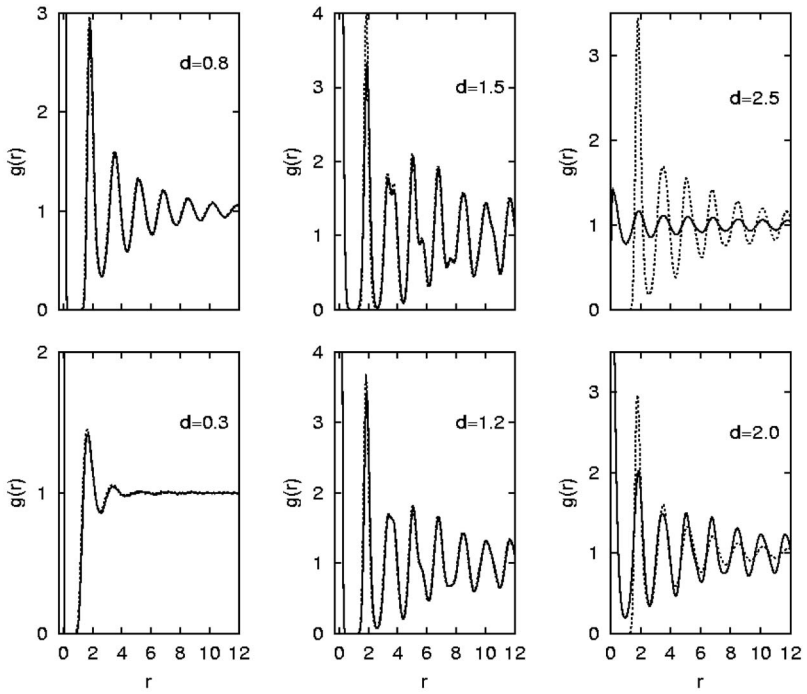

FIG. 1. Intralayer pair correlation function $g_{11}(r)$ denoted by dashed lines and interlayer pair correlation function $g_{12}(r)$ denoted by solid lines, for $\Gamma=150$ and $d=0.3$, 0.8, 1.2, 1,5, 2.0, and 2.5. r and d are in units of a, the Wigner-Seitz radius.

B. Diffusion

The diffusion coefficient D was calculated using Eq. (6); the results are shown in Fig. 2, where we have plotted D (in units of a^2/τ) as a function of the interlayer separation d for values of Γ from 80 to 150. For large d, the diffusion coefficient is that of an isolated two-dimensional one-component plasma interacting with the Coulomb potential. For small d, the formation of electron-hole dipoles which interact weakly increases D by orders of magnitude. For intermediate d, the diffusion coefficient goes through a well-defined minimum. The surprising features of this graph are the steep rise of D for small d, and the considerable range of the interlayer separation $(0<d<0.7)$ in which D is significantly large.

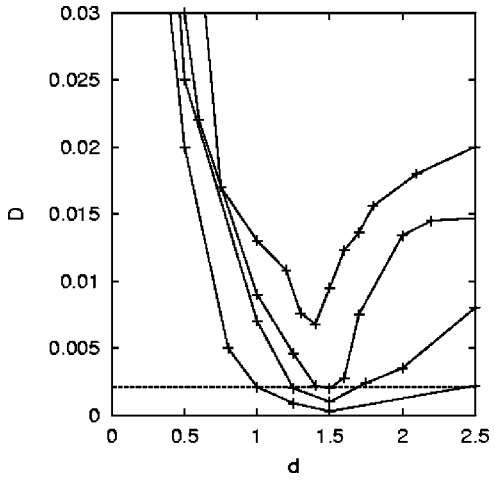

FIG. 2. Dependence of diffusion coefficient D (in units of a^2/τ) on interlayer separation d (in units of a), for $\Gamma=80$, 100, 120, and 150 from top to bottom. The horizontal line at 0.002 is the diffusion coefficient of an isolated two-dimensional OCP at freezing.

The horizontal line at 0.002 indicates the diffusion coefficient of an isolated single layer at $\Gamma=130$; experiments and MD simulations indicate a first-order fluid-solid phase transition in a two-dimensional OCP when Γ is between 120 and 140. If the same criterion is taken as an indication of a fluid-solid phase change in the e-h bilayer, it suggests that this system changes from a fluid to a solid and back to a fluid as the interlayer separation changes from infinity to zero. The range of d values for which the solidlike behavior is observed depends on Γ. For Γ less than about 100, the diffusion never drops below 0.002 for any value of d. This feature will be taken into account later when we discuss the phase diagram of an electron-hole bilayer in the Γ-d plane in Sec. III D.

It is not straightforward to compare our data on the diffusion coefficient with those of Hartmann *et al.*[11] which were obtained through MC simulations. This quantity in an MC calculation can be a useful qualitative indicator of particle mobility in the system but there is no theoretically sound quantitative relationship between it and the real diffusion constant characterizing the physical dynamics of the system, as in an MD calculation. Though the actual values may not match, we find that their general behavior, as a function of Γ and d, is somewhat similar.

The behavior of the diffusion coefficient is quite different in an e-e bilayer. Figure 3 shows the plots of D as a function of d for $\Gamma=100$, for the two systems; the solid line is for the e-h bilayer and the dashed line is for the e-e bilayer. For large d, the two systems behave identically as expected, like a two-dimensional OCP. The minimum in D occurs at quite different values of the interlayer separation. The behavior for small d is dramatically different; the e-e system goes over to a two-dimensional OCP with Γ of $100\sqrt{2}$, while the e-h system goes over to a weakly interacting dipole fluid with a large D.

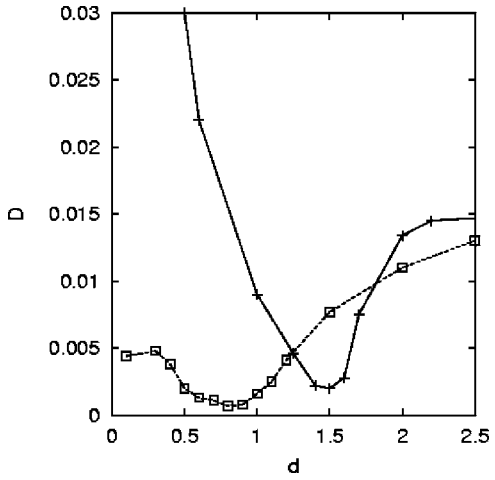

FIG. 3. Comparison of diffusion coefficient D (in units of a^2/τ) as a function of interlayer separation d (in units of a) between the e-e bilayer (dashed line) and the e-h bilayer (solid line), for $\Gamma=100$.

C. Static structure factor

We have computed the static structure factor $S_{11}(q)$ of the intralayer pair distribution function $g_{11}(r)$ with a view of analyzing this quantity as an indicator of a phase transition. Figure 4 shows a typical plot of $S_{11}(q)$ as a function of the wave vector q for $\Gamma=100$, for values of the interlayer separation d from 1.25 to 1.7. The various plots are staggered for clarity. It should be noted that the peak value of $S_{11}(q)$ goes through a maximum as d changes. The horizontal line at 5.2 has been shown to be an indicator of a phase change which will be discussed in the next section on the phase diagram. Here we note that $S_{11}(q)$ exceeds 5.2 for $d=1.4$ and 1.6, while it stays below that number for the other values of d presented.

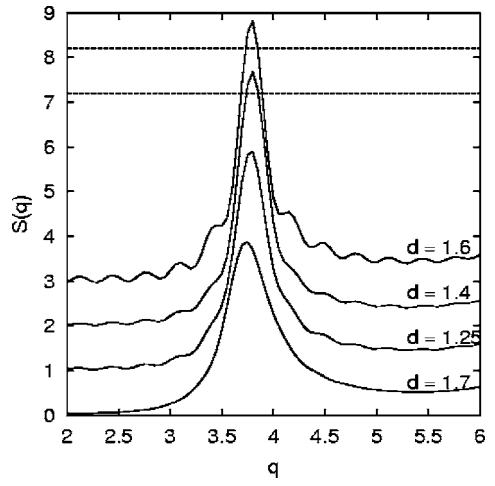

FIG. 4. Intralayer static structure factor $S_{11}(q)$ as a function of the wave vector q (in units of $1/a$), for $\Gamma=100$. The curves are staggered for clarity. The values of d are indicated on the curves. The horizontal line at 5.2 is taken to be the freezing criterion of any two-dimensional system.

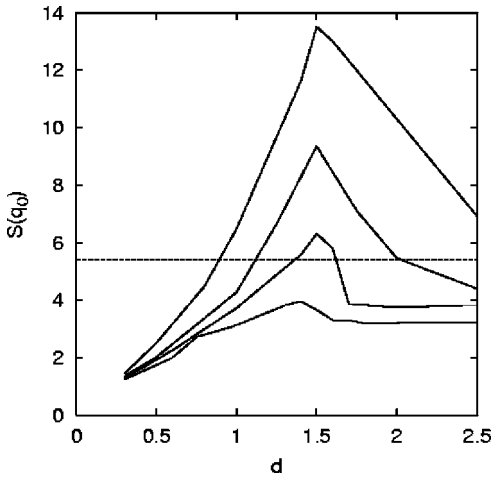

FIG. 5. Amplitude of the main peak, $S_{11}(q_0)$ of the intralayer static structure factor as a function of the interlayer separation d (in units of a), for $\Gamma=80$, 100, 120, and 150 from bottom to top. The horizontal line at 5.2 is taken to be the freezing criterion of any two-dimensional system.

D. Phase diagram

A universal freezing criterion for a three-dimensional system, independent of the interaction potential,[15] states that such a system freezes when $S(q_0)$, the first maximum of the static structure factor, reaches a value of 2.85. A similar analysis of two-dimensional systems with different interaction potentials[12,13] puts this universal value around 5.0. This value is not as definite and accurate as the one for three-dimensional systems, since it has been noted that $S(q_0)$ increases quite rapidly as the freezing state is approached. We have used this criterion to define the phase diagram in e-e bilayers.[5] Figure 5 shows plots of the first maximum of the intralayer structure factor $S_{11}(q_0)$ as a function of d for some representative values of Γ. The horizontal line is drawn at 5.2 as it is a little more consistent with the diffusion data. The states below 5.2 are then fluid states and those above are solidlike states. We note that if Γ is less than about 100, freezing does not occur for any d, since $S_{11}(q_0)$ is always below 5.2. The diffusion coefficient for an isolated two-dimensional OCP is known to be 0.002 at the solidification boundary defined by $\Gamma=130$. Hence based on these two equivalent criteria of diffusion and $S(q_0)$, we have plotted the phase diagram of an electron-hole bilayer and this is shown in Fig. 6. One also notes from the graph that solidification does not occur in an e-h bilayer if d is less than about 0.5; this can be attributed to the formation of weakly interacting stable dipoles for these values of d that prevent a phase change. Our result is shown by a solid line while that of Hartmann *et al.*[11] is shown by a dashed line. It is gratifying to note that the two plots are in very good agreement. Our results also confirm the universality of a freezing criterion that any two-dimensional system or layers of such systems freeze when the peak value of the static structure factor $S_{11}(q_0)$ exceeds 5.2.

The phase diagram of an e-h bilayer is very different from that of an e-e bilayer. A comparison of the two is made in

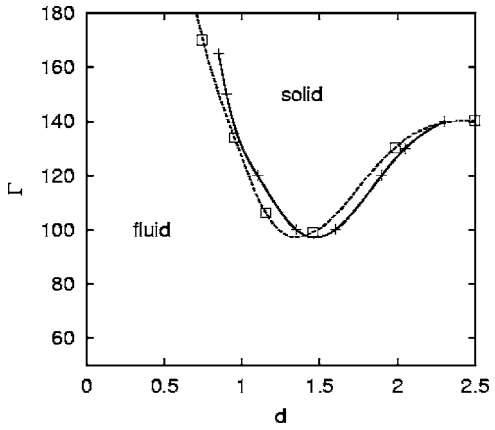

FIG. 6. Phase diagram of a classical, symmetric *e-h* bilayer as a function of the coupling strength Γand the interlayer separation d (in units of a). The points are from diffusion and structure factor data. The dashed line is from Ref. 11.

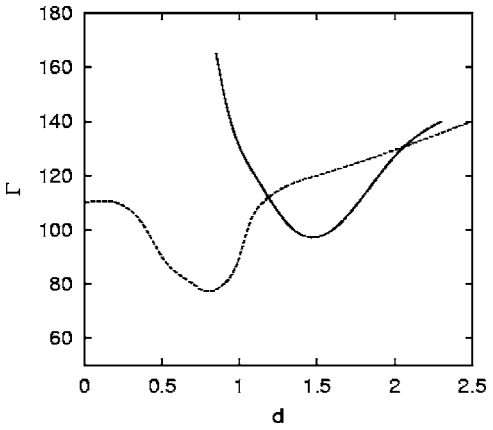

FIG. 7. Comparison of the phase diagrams of a classical, symmetric *e-h* bilayer (solid line) and an *e-e* bilayer (dashed line). Each system is solid above the corresponding line and fluid below.

Fig. 7. As is to be anticipated, the two systems are identical for large interlayer separations. The *e-e* system can sustain a crystalline phase for values of Γ greater than 80 for a limited range of d, while the *e-h* system can do so only for Γ greater than 100. It also shows that an *e-h* system cannot go into a solid phase if d is less than 0.5 (in units of a), for any value of Γ, while the *e-e* system will solidify even at $d=0$, if Γ is more than about 100; note that for the *e-e* system, $\Gamma(d=0) = \sqrt{2}\Gamma(d \approx 3)$.

IV. CONCLUSIONS

We have performed extensive molecular dynamics calculations of a symmetric electron-hole bilayer for various values of the coupling parameter and interlayer separations. We have analyzed, in particular, the diffusion coefficient and the static structure factor, and obtained the phase diagram in the Γ-d plane. The universality of the freezing criterion, that a two-dimensional system or layers of such system freezes when $S(q_0)$, the first maximum of the static structure factor, exceeds about 5.2, is further confirmed by our study. We have also compared our results with those of an electron-electron bilayer and pointed out significant differences between the two systems that arise from the formation of electron-hole dipoles at small interlayer separations.

ACKNOWLEDGMENT

This work was supported in part by a grant from the Academic Research Program (ARP) of the Department of National Defence, Canada.

[1] Z. Donkó and G. J. Kalman, Phys. Rev. E **63**, 061504 (2001).
[2] S. Ranganathan, R. E. Johnson, and K. N. Pathak, Phys. Rev. E **65**, 051203 (2002).
[3] Z. Donkó, P. Hartmann, G. J. Kalman, and K. I. Golden, J. Phys. A **36**, 5877 (2003).
[4] S. Ranganathan and R. E. Johnson, Phys. Rev. B **69**, 085310 (2004).
[5] S. Ranganathan and R. E. Johnson, J. Phys. A **39**, 4595 (2006).
[6] L. Liu, L. Swierkowski, D. Neilson, and J. Szymanski, Phys. Rev. B **53**, 7923 (1996).
[7] G. J. Kalman, V. Valtchinov, and K. I. Golden, Phys. Rev. Lett. **82**, 3124 (1999).
[8] K. I. Golden and G. Kalman, J. Phys. A **36**, 5865 (2003).
[9] I. V. Schweigert, V. A. Schweigert, and F. M. Peeters, Phys. Rev. Lett. **82**, 5293 (1999).
[10] Z. Donkó and G. Kalman, J. Phys. IV **10**, 355 (2000).
[11] P. Hartmann, Z. Donko, and G. J. Kalman, Europhys. Lett. **72**, 396 (2005).
[12] R. C. Gann, S. Chakravarty, and G. V. Chester, Phys. Rev. B **20**, 326 (1979).
[13] S. Ranganathan and K. N. Pathak, Phys. Rev. A **45**, 5789 (1992).
[14] R. E. Johnson, and S. Ranganathan, Phys. Rev. E **63**, 056703 (2001).
[15] J. P. Hansen and L. Verlet, Phys. Rev. **184**, 151 (1969).